

# Facile and novel route for preparation of nanostructured polyaniline (PANi) thin films

D. K. Bandgar · G. D. Khuspe · R. C. Pawar ·  
C. S. Lee · V. B. Patil

Received: 23 August 2012 / Accepted: 4 November 2012 / Published online: 25 November 2012  
© The Author(s) 2012. This article is published with open access at Springerlink.com

**Abstract** Simple and inexpensive single step facile novel chemical route for the preparation of polyaniline (PANi) nanofibers has been reported. These PANi nanofibers are characterized with X-ray diffraction (XRD), Fourier transform infrared (FTIR) spectroscopy, Field emission scanning electron microscopy (FESEM) and Transmission electron microscopy (TEM). Polyaniline nanofibers exhibit amorphous nature as confirmed from XRD and SAED study. Based on FESEM and TEM analysis, the formation of the polyaniline nanofibers with average diameter of about 40 nm was inferred. The presence of characteristic bonds of polyaniline was observed from FTIR spectroscopy technique. Electrical and optical properties revealed that p-type conductivity PANi with room temperature conductivity of  $2.77 \times 10^{-5} (\Omega \text{ cm})^{-1}$  has band gap of 3.40 eV. A blue shift of 0.86 eV with characteristic absorption peak at 441 nm has been attributed due to quantized size of polyaniline nanofibers.

**Keywords** Polyaniline · FESEM · FTIR · TEM · XRD

## Introduction

Nanostructured materials today have immense importance in the field of optoelectronics and biomedical. The experimental and theoretical progress has opened new era of

fundamental physics and chemistry as researchers can make and study artificial analogs of atoms, molecules and crystals. Polymer materials have been widely used in chemical reactions as supports or catalysts due to their flexible applicability.

An attractive subject of research was initiated with the discovery of conducting polymers (conjugated polymers). Among the most commonly studied conducting polymers is polyaniline, also known as highly tunable and air-stable organic conducting polymer with good environmental stability, which can be produced as bulk powder, cast films or fibers. This, in conjunction with the feasibility of low cost monomer, large-scale production, redox reversibility serves to further enhance its favorable properties and makes it an ideal candidate in many applications. This could greatly widen its applicability in multidisciplinary areas such as electrical, electronics, thermoelectric, electrochemical, electromagnetic, electromechanical, electro-luminescence, electrorheological, chemical, membrane and sensors (Borole et al. 2006; Jacinth Mispa et al. 2011; El Ghanem et al. 2006; Pawar et al. 2009; Chougule et al. 2012a). The PANi can mainly occur in three forms, including so-called fully reduced pale yellow-colored leucoemeraldine (LEB), the partially oxidized green-colored emeraldine base (EB) and fully oxidized bluish-violet colored pernigraniline (PEB). The electrical and optical properties of the polyaniline vary with the different oxidation states and different forms. It can be configured or controlled to conduct across a wide range, from being utterly non-conductive for insulation use to highly conductive for other electrical purposes (Patil et al. 2012). The emeraldine base is more stable form in air at ambient temperature.

The available literature revealed different methods to synthesize PANi including electrochemical (Patil et al. 2009), template (Raut et al. 2012a), enzymatic (Kobayashi

D. K. Bandgar · G. D. Khuspe · V. B. Patil (✉)  
Materials Research Laboratory, School of Physical Sciences,  
Solapur University, Solapur 413255, MS, India  
e-mail: drvbpatil@gmail.com

R. C. Pawar · C. S. Lee  
Department of Materials Engineering,  
Hanyang University, Ansan 426-791, South Korea

et al. 2001), plasma (Nastase et al. 2005), photo (Kobayashi et al. 1998), subdivision of chemical polymerization into heterophase (Vidotto et al. 1969), solution (Kuramoto and Tomita 1997), interfacial (Dallas et al. 2007), seeding (Xing et al. 2006), metathesis (Zhang et al. 2009), self-assembling (Bahgat et al. 2003) and sonochemical (Jing et al. 2006) polymerizations.

The unnecessary formation of precipitation, waste of material in many of the above reported methods that are money, time and energy consuming, cumbersome along with needed sophisticated instruments for controlling various parameters may put restrictions on the commercial synthesis of materials. These can be avoided by facile and novel in situ chemical route which results into entailed thin film form of the deposit at room temperature.

Khuspe et al. reported microstructural and optical properties of nanostructured polyaniline in semiconducting form PANi (EB) by chemical oxidation polymerization method for ammonia gas sensing applications (Khuspe et al. 2012).

Following reasons strongly portrays our in situ chemical route as facile, novel and efficient among the rest deposition methods. It is relatively simpler and cheaper method that has emerged as one of the recent soft chemical solution methods. It is advantageous due to layer-by-layer growth and comprises excellent material utilization efficiency, good control over deposition process along with film thickness and specifically convenient for large area deposition on virtually any type of substrate. The in situ preparation of PANi film results in pinhole free and uniform deposits, since the basic building blocks are ions instead of atoms. Oxidation and corrosion of metallic substrates can be avoided as deposition is carried at or near room temperature (Chougule et al. 2011; Raut et al. 2012b).

In this work, a systematical investigation on the oxidative chemical polymerization of aniline is made as simple as possible by facile lucrative in situ chemical route at room temperature, which results in good quality, uniform,

well-adherent, porous and nanofibrous-structured semiconducting polyaniline (PANi-EB) in the thin film form feasible for large area deposition. Our efforts are focused onto development of easiest and cheapest synthesis route for the preparation of PANi (EB) commercially, so that to achieve compatibility in applications. Further, in situ grown films are characterized for study of structural, morphological, optical and electrical transport properties.

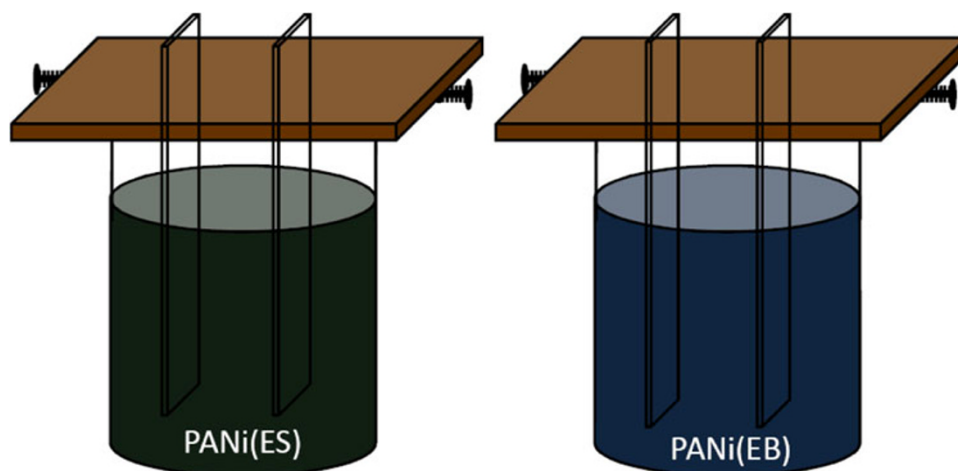
### Experimental details

Aniline monomer and other reagents, such as dopant HCl, oxidant (ammonium peroxydisulfate, APS) were used as received [AR grade, Sd. fine Chem. Ltd, Mumbai (India)]. A typical in situ polymerization technique was employed to synthesize PANi thin films onto glass substrate (Fig. 1). The polymerization procedure was as follows: PANi was prepared by chemical oxidation process using aqueous acidic solution of 0.2 M aniline ( $C_6H_5NH_2$ ) + 0.1 M APS + 0.2 M HCl.

The reaction mixture was kept for 3 h at the room temperature, briefly stirred and left at rest to polymerize for 5 h. The green precipitate occurred. The resultant product was PANi in emeraldine salt form, i.e., PANi (ES). To obtain emeraldine base form of PANi, dedope ES form of PANi with 0.1 M  $NH_4OH$  solution and pre-cleaned glass substrates were dipped in the beaker. The solution was briefly stirred and left at rest to polymerize at room temperature. The blue thin layer of PANi deposited on the glass substrate after 3 h; thus, finally obtained film of insulating polyaniline (EB). The resulting PANi film was washed under distilled water to remove the low molecular weight organic intermediates, oligomers, etc. and dried at the room temperature and used for further studies.

Thickness of deposited PANi thin film was measured using fully computerized AMBIOS Make XP-1 surface

**Fig. 1** The schematic of in situ method for deposition of PANi on the substrate



profiler with 1 Å vertical resolution and found to be 110 nm. The XRD pattern was taken under the conditions of 40 kV and 100 mA with  $\text{CuK}_\alpha$  radiations ( $K = 1.5426 \text{ \AA}$ ) using Philips PW 3710, X-ray diffractometer (XRD) for structural studies. The surface morphology and grain size of the PANi nano fiber have been characterized by FESEM (XL30 ESEM-FEG) and transmission electron microscopy (Philips CM-30 TEM unit, point resolution = 2.4 Å) with acceleration voltage of 300 kV coupled with EDAX-DX-4 analyzer. The AFM images were obtained using a scanning probe microscope (SPM-Solver P47, NTMDT, Russia) in contact mode. The FT-IR spectrum of the sample was collected using a 'Perkin Elmer, FT-IR Spectrum one' unit. UV-Vis absorption spectra were recorded on a Systronic spectrophotometer-119 with glass substrate as a reference in the wavelength range of 300–1,000 nm. The electrical transport properties were studied using two probe techniques in 300–500 K temperature range.

## Results and discussion

### Reaction mechanism

Chemical polymerization is a simple and fast process with no need for special instruments. During the chemical polymerization of aniline, electroneutrality of the polymer matrix is maintained by incorporation of anions from the reaction solution. These counter ions are usually the anions of the chemical oxidant or reduced product of oxidant. In present investigation ammonium persulfate (APS) is used as chemical oxidant for chemical polymerization. The possible reaction mechanism for in situ chemical polymerization of polyaniline is given as follows:

For preparation of semiconducting polyaniline (polyaniline base) by novel in situ chemical polymerization, reaction mixture contains the solution of 0.2 M aniline prepared in 1 M hydrochloric acid which serves as a cationic precursor at room temperature with  $\text{pH} \approx 1$ . Ammonium persulfate in double distilled water acts as oxidizing agent at room temperature. 0.1 M ammonium persulfate solution in water ( $\text{pH} \approx 3$ ) at room temperature (as anionic precursor solution) was suddenly added into the above solution. Here, anilinium cations are the prevailing monomer species. Further reaction is followed by the immersion of the glass substrate in the solution; intuitively wherein, the oxidative chemical polymerization reaction with monomer species of anilinium cations occurs. First, oxidation of anilinium cation monomer species takes place by persulfate anions. The two electron oxidation reaction of anilinium cation by persulfate anion, leading to generation of aniline nitrenium ( $\text{C}_6\text{H}_5\text{NH}^+$ ) cation is explained in Scheme 1b (Trivedi 1997; Konyushenko et al. 2006). An

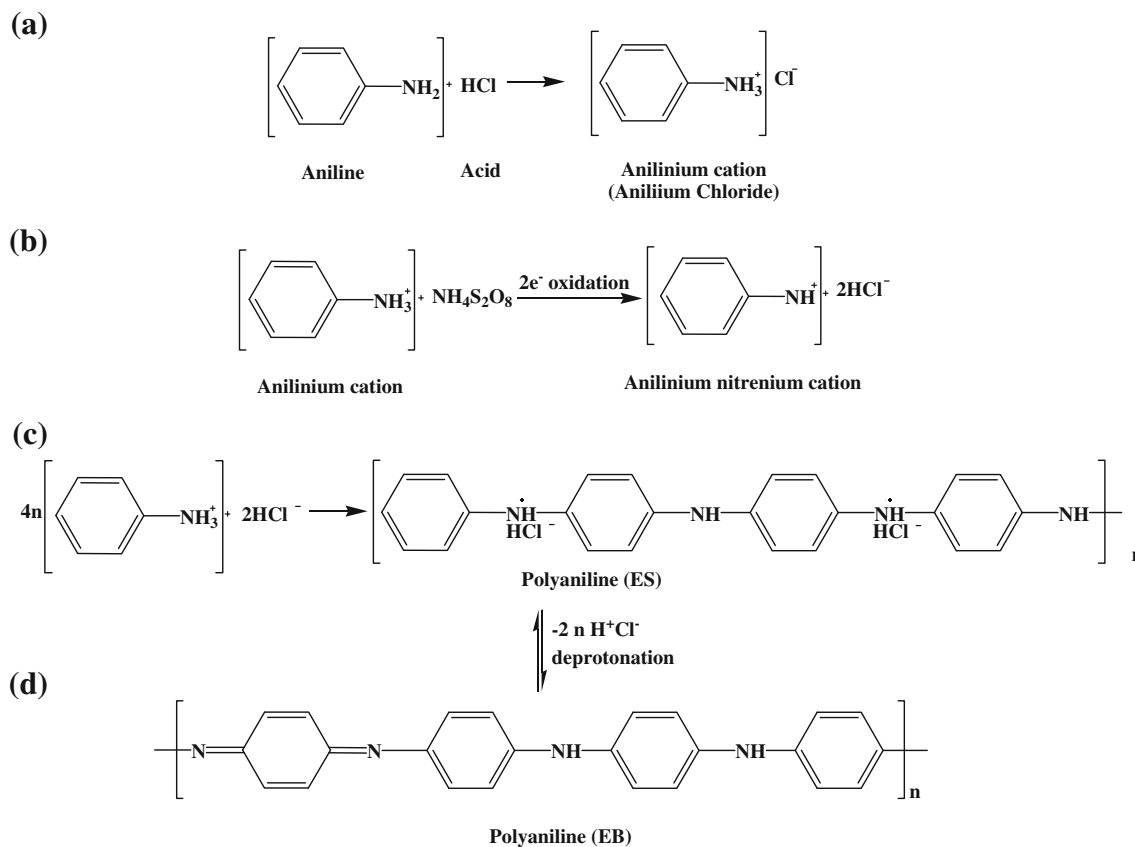
efficient polymerization of aniline is achieved in an acidic media wherein, aniline exists as an anilinium cation ( $\text{C}_6\text{H}_5\text{NH}_3^+$ ) (Trivedi 1997). The anilinium chloride produced by the reaction of aniline and hydrochloric acid (Khuspe et al. 2012; Konyushenko et al. 2006; Perrin 2003) acts as a cation source and can be explained by the reaction shown in Scheme 1a. When substrate is immersed in the above solution, these anilinium cations get adsorbed on the substrate due to the attractive force between surface of the substrate and ions in the solution. These forces may be cohesive forces or van der Waals forces or chemical attractive forces. And second, adsorbed aniline nitrenium cations ( $\text{C}_6\text{H}_5\text{NH}^+$ ) react with hydrochloride anions ( $\text{HCl}^-$ ) leading into the formation of dark green-colored PANi (emeraldine) hydrogen chloride as shown in Scheme 1c. Anilinium cation in the form of anilinium chloride is produced after reaction of aniline with hydrochloric acid and further oxidized with ammonium persulfate at room temperature to produce PANi (emeraldine) hydrochloride (Konyushenko et al. 2006). Protonated polyaniline (PANi hydrochloride) when treated with ammonium hydroxide converts to a semiconducting blue emeraldine base ( $\text{pH} \approx 8$ ) layer with only a few nanometer thickness as shown in Scheme 1d.

### Structural analysis

The crystallinity and orientation of conducting polymers have been of much interest because highly ordered systems can display metal-like conductive states (Li et al. 1993). Figure 2 shows a typical XRD pattern for polyaniline thin films on glass substrates. Figure 2 also displays broad diffraction peak corresponding to  $2\theta = 25.30^\circ$  (110) which is consistent with XRD patterns of the polyaniline observed by other groups (Chaudhari and Kelkar 1996, 1997). The peak at  $2\theta = 25.30^\circ$  may be ascribed to periodicity parallel to the polymer chain (Moon et al. 1989). The peak at  $2\theta = 25.30^\circ$  may also represent the characteristic distance between the ring planes of benzene rings in adjacent chains or the close contact interchain distance (Pouget et al. 1995). The characteristic broadening of the observed peaks implies that the films are nanocrystalline.

### Microstructural analysis

The two-dimensional surface morphology of the polyaniline thin films has been studied using FESEM images. Figure 3 shows the FESEM images of polyaniline thin film. Polyaniline surface with fussy fibers is clearly seen from FESEM images. FESEM image confirms the interconnected polyaniline nanofibers. The fibers are relatively smooth with randomly distributed over the substrate and these nanofibers are with approximately average diameter



**Scheme 1** Reaction mechanism for in situ chemically deposited PANi. **a** The reaction of aniline with hydrochloric acid gives anilinium cations in the form of anilinium chloride. **b** The oxidative chemical reaction of anilinium cations by persulfate anions of ammonium persulfate leading to generation of aniline nitrenium

cations. **c** The next to oxidative chemical reaction, aniline nitrenium cations react with hydrogen chloride anions to form PANi (emeraldine) salt and **d** polyaniline (emeraldine) salt is deprotonated in the alkaline medium to polyaniline(emeraldine) base

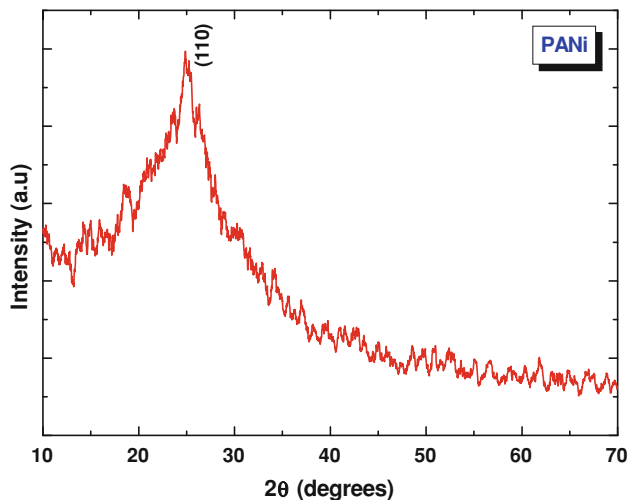


**Fig. 2** X-ray diffraction patterns of PANi (EB) film

of 40 nm. The micrograph shows the interconnected nanofibers forming web-like structure with hollow cavities which are highly porous. The porous nature of the polyaniline makes it a potential candidate for various

surface-related applications such as gas sensors and energy storage devices.

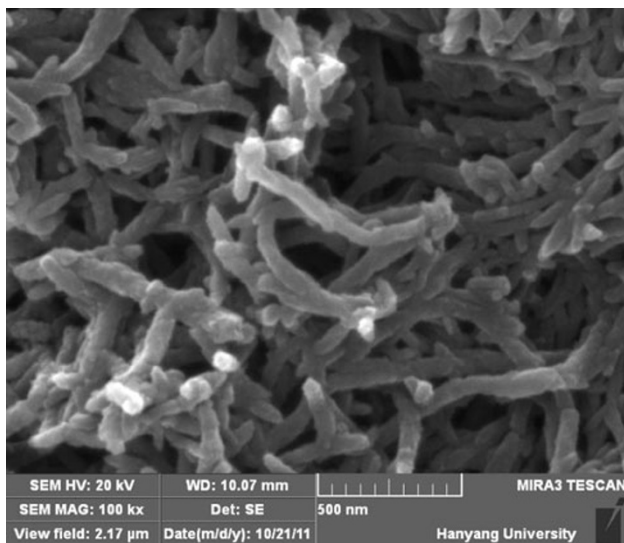
The morphology of PANi (EB) consisting strongly interconnected fibers was further studied with high magnified TEM analysis (Fig. 4a). It shows that the film composed of interconnected nanofibers of average diameter around 40 nm, which is in consistent with grain size calculated from FESEM studies.

Figure 4b shows corresponding selected area electron diffraction (SAED) pattern of polyaniline nanofibers. The blurred bright electron diffraction rings show that the polyaniline film is amorphous or poorly crystalline, supported to X-ray diffraction results (Fig. 2).

The two- (2D) and three- (3D) dimensional surface topology of the PANi thin films were investigated using atomic force microscopy (AFM). Figure 5a, b shows the 2D and 3D AFM micrographs of PANi thin films, respectively. From the micrograph (5a), total coverage of the substrate with interconnected fibers is seen. From the 3D micrograph (Fig. 5b), it is seen that the film consists of distributed cuboidal shaped interconnected fibers with some visible voids, which is consistent with FESEM image.

## FTIR analysis

The FT-IR spectrum of the PANi in the range 500–4,000  $\text{cm}^{-1}$  is shown in Fig. 6. Primly nine absorption peaks are observed. The broad band at 3,428  $\text{cm}^{-1}$  was assigned to the free N–H stretching vibrations of secondary amines (Zeng and Ko 1998; Trchova et al. 2006). The smaller one peak at 2,921  $\text{cm}^{-1}$  is characterized to the vibration associated with the  $\text{NH}^{2+}$  part in the  $-\text{C}_6\text{H}_4\text{NH}^{2+}\text{C}_6\text{H}_4-$  group (Palaniappan and Narayana 1994; Quillard et al. 2001). The band at 1,559  $\text{cm}^{-1}$  is due to quinoid ring deformations of aromatic ring. The peaks at 1,470 and 1,292  $\text{cm}^{-1}$  are the results of the stretching vibrations of C N<sup>+</sup> and C–N,



**Fig. 3** FESEM micrograph of PANi (EB) thin film

respectively (Kang et al. 1998). The peaks at 1,121 and 801  $\text{cm}^{-1}$  are attributed to the aromatic C–H bending in the plane and out of the plane for the 1, 4-disubstituted aromatic ring (Çolak and Sökmen 2000; Liu et al. 2002). The band at 499  $\text{cm}^{-1}$  is attributed to S–C stretching vibration mode, indicating the presence of the chloro group which supports formation of emeraldine PANi hydrogen chloride. Chloronate groups interact with protonated imine nitrogen in neighboring chains and stabilize the PANi. All the above observed absorption characteristics confirm the formation of PANi.

## Electrical transport properties

### DC electrical conductivity

The dc electrical conductivity of polyaniline film was measured in the 300–500 K temperature range and their temperature dependence can be fitted to a usual Arrhenius equation:

$$\sigma = \sigma_0 \exp(-E_{a\sigma}/KT) \quad (1)$$

where,  $\sigma$  is the conductivity at temperature  $T$ ,  $\sigma_0$  is a constant,  $k$  is the Boltzmann constant,  $T$  is the absolute temperature and  $E_a$  is the activation energy. The activation energy represents the location of trap levels below the conduction band. The temperature dependence of dc electrical conductivity of PANi (EB) (Fig. 7) showed two distinct conduction regions corresponding to two different conduction mechanisms; one, a grain boundary scattering limited and second a variable range hopping (Raut et al. 2012b; Patil et al. 2011). From Fig. 7, it is observed that conductivity obeys Arrhenius behavior indicating a

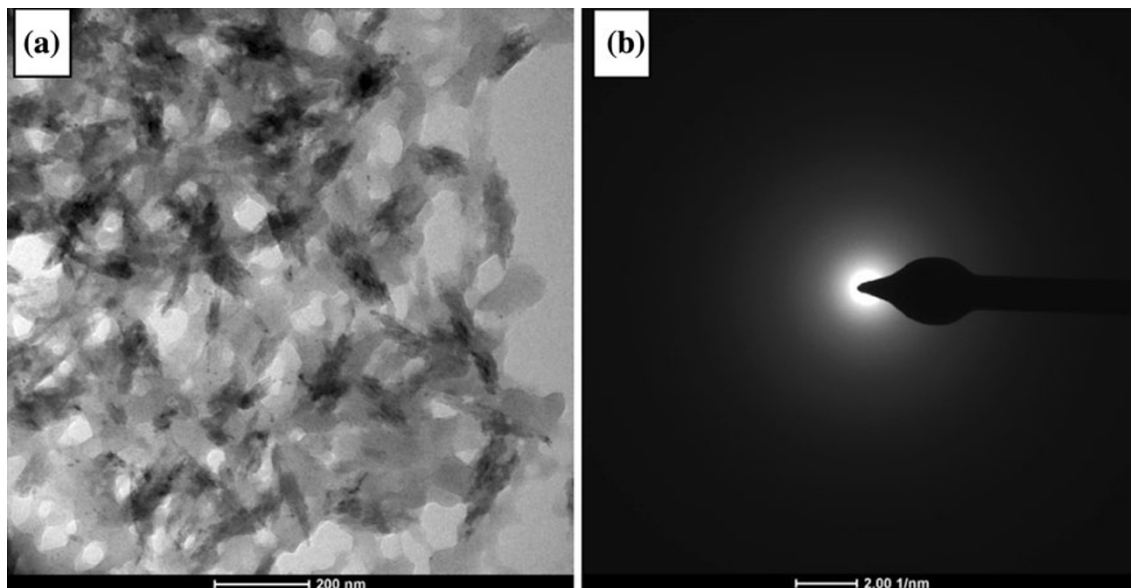


**Fig. 4** a TEM image of polyaniline nanofibers, b SAED pattern of corresponding polyaniline nanofibers

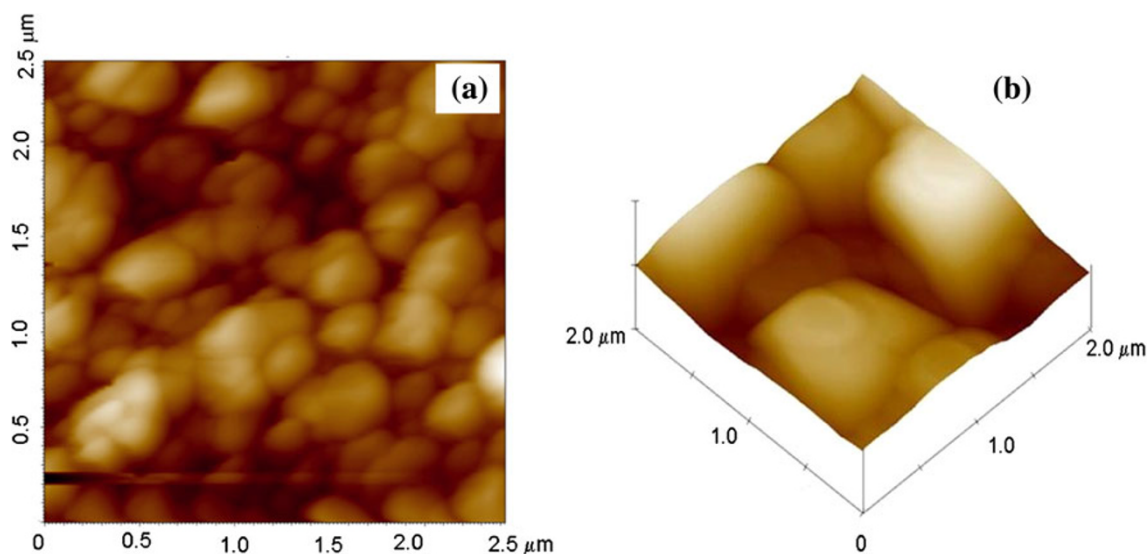


**Fig. 5** The 2D **a** and 3D **b** AFM images of polyaniline thin film

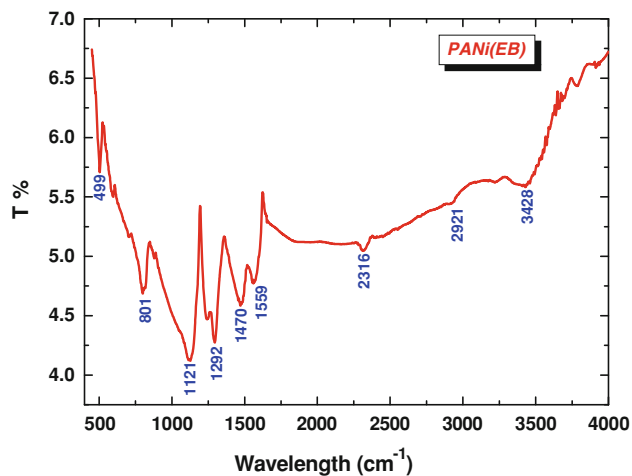


**Fig. 6** FTIR spectra of PANi (EB) thin film

semiconducting transport behavior. The activation energies of an electrical conduction have been computed for both high and low temperature regions (from Fig. 7) and are 0.66 and 0.24 eV, respectively.

#### Thermo-emf measurement

The temperature difference causes a transport of carriers from the hot to cold end and thus creates an electric field, which gives rise to a thermally generated voltage. The thermo-emf property of polyaniline was measured as a function of temperature in the 300–500 K temperature range and is shown in Fig. 8.

The thermo-emf developed between two ends showed that the polyaniline is a p-type electrical conductivity

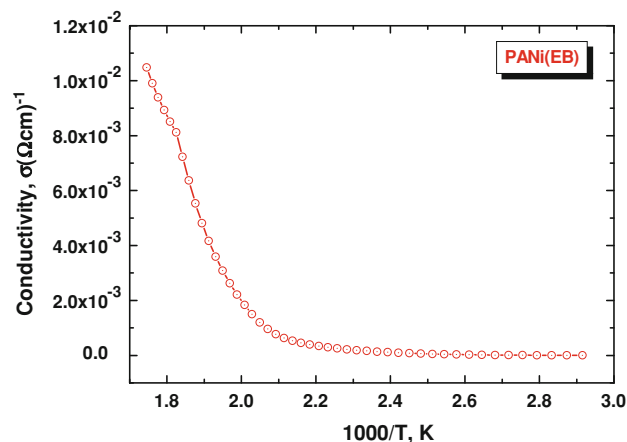


**Fig. 7** Plot of dc electrical conductivity ( $\sigma$ ) versus inverse temperature of PANi (EB) film

material and that the holes contribute to TEP similar to the results reported earlier (Chougule et al. 2012b). The thermo-emf increased linearly with increasing temperature. Chougule et al. (2012c) have also reported that the thermoelectric power increases with increase in temperature for organo-soluble polyaniline doped with HCl. The TEP results indicate that the conductivity mechanism of the polymer is controlled by the large polaron hopping model.

From the experimental observations it appeared that the temperature dependence of thermo power is approximately linear in the low temperature region whereas it deviated from the linear behavior at higher temperature and obeys power law dependence of the temperature. The non-linearity of the plots indicates non-degeneracy of the material whose thermoelectric power is proportional to nth power of

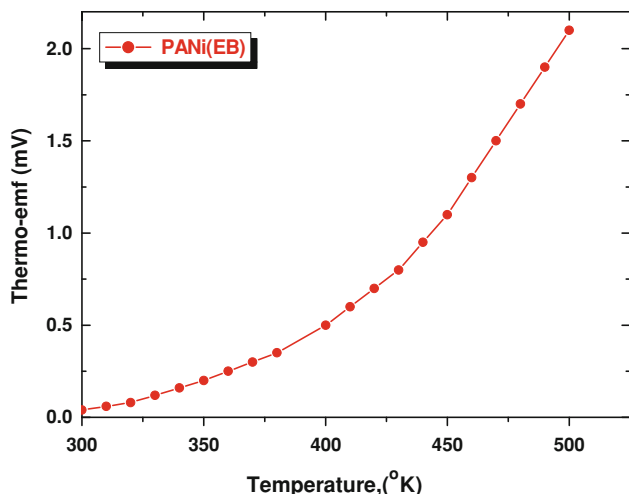


**Fig. 8** Variation of thermo-emf with temperature of polyaniline thin film

the absolute temperature. For such semiconductors thermoelectric power is a weak function of the temperature and can be represented as (Sekkina and Tawfik 1995):

$$P = -K/e[r + 5/2] + \ln \{2(2\pi m_d^* kT)^{3/2} / nh\}^3 \quad (2)$$

where  $P$  is thermoelectric power in  $\text{mVK}^{-1}$ ,  $A = r + 5/2$  is a thermoelectric factor that depends on the various scattering mechanisms,  $m_d^*$  is the density of states effective mass and  $n$  is the carrier concentration. Equation (2) can be solved for appropriate values of  $A$  and  $m_d^*$ , and carrier concentration ( $n$ ) were calculated for all the samples at different temperatures. The charge carrier motilities ( $\mu$ ) were determined using the standard relation.

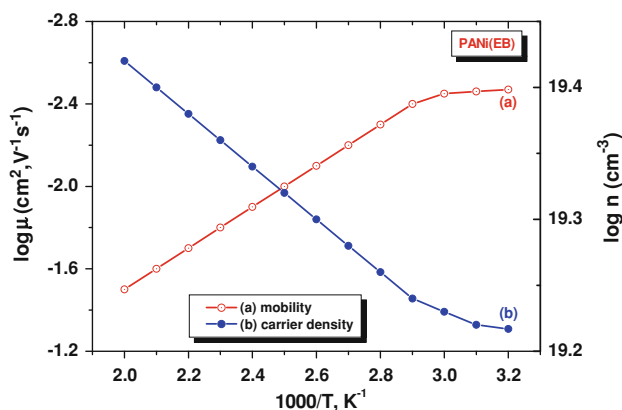
$$\mu = \sigma / n \times e \quad (3)$$

Figure 9 is a plot of the carrier concentration ( $n$ ) and mobility ( $\mu$ ) as a function inverse absolute temperature. It is seen that the carrier concentration and mobility are dependent functions of the temperature. These variations are analogous with that of the electrical conductivity variations. The observed value of  $n$  and  $\mu$  is of the order of  $10^{19} \text{ cm}^{-3}$  and  $10^{-6} \text{ cm}^2 \text{ V}^{-1} \text{ s}^{-1}$ . Further, the mobility increased with the applied temperature suggesting the presence of scattering mechanism associated with the inter grain barrier height as proposed by Petriz (1956).

The temperature-dependent grain boundary mobility is related to the grain boundary potential as (Micocci et al. 1995):

$$\mu = \mu_0 \exp(-\Phi_b/kT) \quad (4)$$

where  $\Phi_b$  is the inter grain barrier potential and  $\mu_0$  is the pre exponential factor. The inter grain barrier potential is therefore determined from the variation of the  $\log \mu T^{1/2}$



**Fig. 9** Plot of  $\log n$  and  $\log \mu$  as a function of inverse temperature for PANi thin film

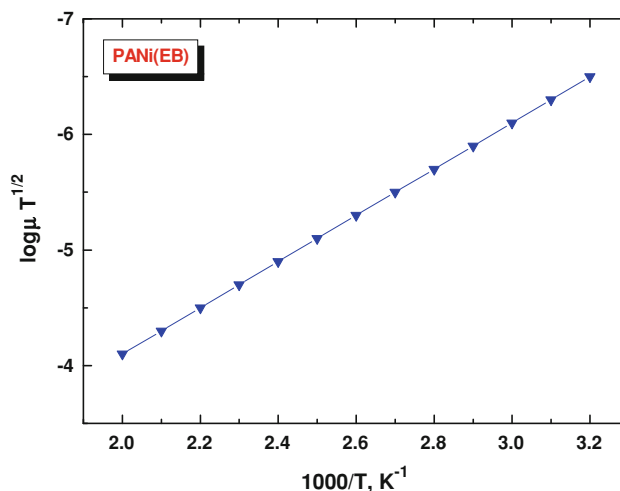


**Fig. 10** Determination of intercrystalline barrier height for PANi film

versus  $1/T$  as suggested by Micocci et al. (1963). This is shown in Fig. 10 and its typical value is 0.49 eV.

From the observed values of the activation energies of an electrical conduction ( $E_{a\sigma}$ ) and the electron density ( $E_{an}$ ), the relation

$$E_{a\sigma} = E_{an} + \Phi_b \quad (5)$$

holds good. This is expected from the interrelationship between the electrical conductivity, carrier density and mobility (Patil et al. 2011; Raut et al. 2012c; Sekkina and Tawfik 1995; Petriz 1956; Micocci et al. 1995).

#### Thermo-gravimetric analysis (TGA) and differential thermal analysis (DTA)

Thermo gravimetric analysis and DTA of polyaniline in powder form were carried out to study endothermic and

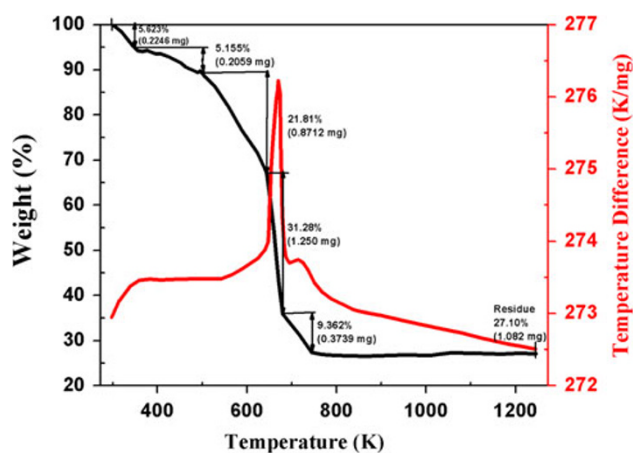


**Fig. 11** TGA–DTA spectra of polyaniline thin film in air atmosphere

exothermic reactions at a heating rate of 10 K/min in air atmosphere from 273 to 1,273 K as shown in Fig. 11.

The thermal evolution in air atmosphere takes place in four consecutive stages corresponding to weight losses in which the inflection point coincides with the temperature of the endotherms and exotherms in DTA trace. The weight loss of polyaniline begins at 323 K. The weight loss commencing at around 373 K is assigned to the loss of initially present water molecules (Duval 1963). Rapid weight loss is found in temperature range of 493–743 K due to the consequence of structural decomposition of the polymer and elimination of dopant molecules. After 743 K, the DTA trace is stable with no further weight loss is observed. This indicates that the polyaniline is stable up to 323 K and then polyaniline starts degrading slowly. The smooth thermogram shows only one exothermic peak at 668 K, where thermal decomposition of polyaniline takes place. Ansari and Keivani (2006) obtained the similar behavior of polyaniline prepared by cyclic voltammetry and reported that the polyaniline prepared by cyclic voltammetry is highly thermal stable than that of prepared by potentiostatic mode.

#### Optical absorption studies

Figure 12 shows the variation of optical absorbance ( $\alpha t$ ) with incident photon wavelength ( $\lambda$ ) of the polyaniline thin film having thickness of 110 nm. The UV–Vis–NIR absorption spectrum of PANi film shows two sharp absorptions: one with maximum at 441 nm ( $\approx 3.4$  eV)  $\pi$ – $\pi^*$  transition of benzenoid ring and another at 652 nm ( $\approx 2.04$  eV) corresponding to molecular exciton transition. This is due to the oxidation states of the PANi (de Albuquerque et al. 2004).

As seen in figure, peak generally preferred to as the excitonic peak, which is the typical characteristic of

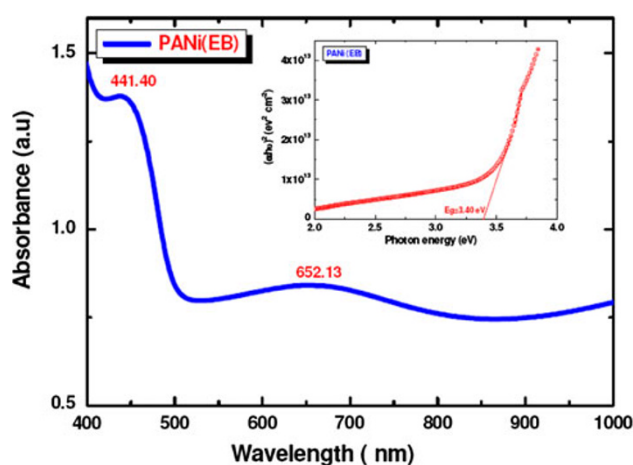


**Fig. 12** The plot of absorption ( $\alpha t$ ) with wavelength ( $\lambda$ ) of PANi thin film on glass substrate

nanocrystallites, follows the absorption at 425–450 nm. The absorbance band approximately at 440 nm has been reported earlier and may be attributed to the excitation to the polaron band (Wang and Herron 1991). For semiconductor materials, the quantum size effect is expected if the semiconductor dimension becomes smaller than the Bohr radius of the exciton and the absorption edge is red shifted. The theory of optical absorption gives the relationship between the absorption coefficient ( $\alpha$ ) and the photon energy ( $h\nu$ ) for direct allowed transition can be written as:

$$\alpha h\nu = \alpha_0 (h\nu - E_g)^{1/2} \quad (6)$$

where  $\alpha_0$  is a constant,  $h\nu$  is the photon energy and  $E_g$  is the band gap of the material. Inset of Fig. 12 shows the variation of  $(\alpha h\nu)^2$  with incident photon energy ( $h\nu$ ), the band gap,  $E_g$ , was determined. The band gap was found to be 3.40 eV which is lower than earlier reported by Sajeev et al. (2006) (3.65 eV) and higher than earlier reported by Pawar et al. (2011) (2.54 eV), showing a blue shift of 0.86 eV. This is attributed to the size quantization of nanofibered polyaniline thin films. It is well known that the band gap energies for the well-crystallized thin films are comparable to those of crystallized bulk materials, where as in amorphous and/or nanocrystallized forms, the band gap energies are higher than those of the corresponding bulk materials.

#### Conclusion

In conclusions, a direct one-step and environmentally friendly simple, inexpensive facile and novel chemical synthesis method has been developed to produce fussy polyaniline nanofibers at room temperature.

This may be helpful for commercially synthesis of polyaniline. Study of physico-chemical characteristics with



XRD, FT-IR, FESEM, TEM, SAED, AFM, optical and electrical techniques confirmed preparation of amorphous, nanostructure, wide optical band gap and low resistivity of p-type PANi thin film. The in situ chemical method is efficient and constructive for deposition of fused nanofibers like PANi films onto substrates of different area with feasibility, at expense of small amount of initial ingredients.

**Acknowledgments** Authors (VBP) are grateful to DAE-BRNS, for financial support through the Scheme No. 2010/37P/45/BRNS/1442.

**Open Access** This article is distributed under the terms of the Creative Commons Attribution License which permits any use, distribution, and reproduction in any medium, provided the original author(s) and the source are credited.

## References

- Ansari RM, Keivani EB (2006) Polyaniline conducting electroactive polymers: thermal and environmental stability studies. *J Chem* 3:202–217
- Bahgat AA, Sayyah SM, Abd-Elsalam HM (2003) Study of ferroelectricity in polyaniline. *Int J Polym Mater* 52:499–515
- Borole DD, Kapadi UR, Mahulikar PP, Hundiware DG (2006) Synthesis of nano polyaniline and poly-o-anisidine and applications in alkyd paint formulation to enhance the corrosion resistivity of mild steel. *Polym Plast Technol Eng* 45:667
- Chaudhari HK, Kelkar DS (1996) X-ray diffraction study of doped polyaniline. *J Appl Polym Sci* 62:15–18
- Chaudhari HK, Kelkar DS (1997) Investigation of structure and electrical conductivity in doped polyaniline. *Polym Int* 42:380–384
- Chougule MA, Pawar SG, Patil SL, Raut BT, Patil VB (2011) Polypyrrole thin films: room temperature ammonia sensor. *IEEE Sensor J* 11:2137–2141
- Chougule MA, Patil SL, Pawar SG, Raut BT, Godse PR, Sen S, Patil VB (2012a) Facile and efficient route for preparation of Polypyrrole–ZnO nanocomposites: microstructural optical and charge transport properties. *J Appl Polym Sci*. doi:10.1002/app36475
- Chougule MA, Sen S, Patil VB (2012b) Polypyrrole–ZnO hybrid sensor: effect of camphor sulfonic acid doping on physical and gas sensing properties. *Synth Metals* 162:1598–1603
- Chougule MA, Sen S, Patil VB (2012c) Polypyrrole–ZnO nanohybrids: effect of CSA doping on structure, morphology and optoelectronic properties. *J Appl Nanosci*. doi:10.1006/s13204-012-0149-x
- Çolak N, Sökmen B (2000) Doping of chemically synthesized polyaniline. *Des Monomers Polym* 3:181–189
- Dallas P, Stamopoulos D, Boukos N, Tzitzios V, Niarchos D, Petridis D (2007) Characterization, magnetic and transport properties of polyaniline synthesized through interfacial polymerization. *Polymer* 48:3162–3169
- de Albuquerque JE, Mattoso LHC, Faria RM, Masters JG, MacDiarmid AG (2004) Study of the interconversion of polyaniline oxidation states by optical absorption spectroscopy. *Synth Met* 146:1–10
- Duval C (1963) Inorganic thermogravimetric analysis. Elsevier, Amsterdam, p 315
- El Ghanem HM, Attar H, Sayid Ahmad H, Abduljawad S (2006) Dielectric spectroscopy of conducting polyaniline polymer. *Int J Polym Mater* 55:663–679
- Jacynth Mispa K, Subramaniam P, Murugesan R (2011) Oxidative polymerization of aniline using zirconium vanadate, a novel polyaniline hybrid ion exchanger. *Des Monomers Polym* 14:423–432
- Jing XL, Wang YY, Wu D, She L, Guo Y (2006) Polyaniline nanofibers synthesized by rapid mixing polymerization. *J Polym Sci Polym Chem* 44:1014
- Kang ET, Neoh KG, Tan KL (1998) Polyaniline: a polymer with many interesting intrinsic redox states. *Prog Polym Sci* 23:277–324
- Khuspe GD, Bandgar DK, Patil VB (2012) Fussy nanofibrous network of polyaniline (PANi) for NH<sub>3</sub> detection. *Synth Metals* 162:1822–1827
- Kobayashi N, Teshima K, Hirohashi R (1998) Conducting polymer image formation with photoinduced electron transfer reaction. *J Mater Chem* 8:497–506
- Kobayashi S, Uyama H, Kimura S (2001) Synthesis and chemical properties of polyphenols with oligoaniline pendant groups. *Chem Rev* 101:3793
- Konyushenko EN, Stejskal J, Sedekov I, Trchov M, Sapurina I, Cieslar M, Prokes J (2006) Evolution, performance, ageing and reincarnation of polyaniline. *Polym Int* 55:31
- Kuramoto N, Tomita A (1997) Chemical oxidative polymerization of dodecylbenzenesulfonic acid aniline salt in chloroform. *Synth Met* 88:147–151
- Li Q, Cruz L, Philips P (1993) Low-temperature heat capacities of polyaniline and polyaniline polymethylmethacrylate blends. *Phys Rev B* 47:1840
- Liu H, Hu XB, Wang JY, Boughton RI (2002) Structure, conductivity, and thermo power of crystalline polyaniline synthesized by the ultrasonic irradiation polymerization method. *Macromolecules* 35:9414–9419
- Micocci G, Tepore A, Rella R, Siciliano P (1995) Electrical and optical characterization of electron beam evaporated In<sub>2</sub>Se<sub>3</sub> thin films. *Phys Status Solidi A* 148:343–431
- Moon YB, Cao Y, Smith P, Heeger AJ (1989) Composite films of nanostructured polyaniline with poly(vinyl alcohol). *Polym Commun* 30:196
- Nastase C, Nastase F, Dumitru A, Ionescu M, Stamatini I (2005) Thin film composites of nanocarbons-polyaniline obtained by plasma polymerization technique. *Compos A Appl Sci Manuf* 36:481–485
- Palaniappan S, Narayana BH (1994) Composition and spectral studies of polyaniline salts. *Polym Adv Technol* 5:225–230
- Patil VB, Pawar SG, Patil SL, Sood AK (2009) Optoelectronic and microstructural properties of PANi (EB)-CSA<sub>x</sub> polymer thin films by novel spin coating method. *Orient J Chem* 25(4):945–952
- Patil SL, Pawar SG, Chougule MA, Sen S, Patil VB (2011) Nanocrystalline ZnO thin films: Effect of annealing on microstructural and optoelectronic properties. *J Alloys Compd* 509:10055–10061
- Patil SL, Pawar SG, Chougule MA, Raut BT, Godse PR, Sen S, Patil VB (2012) Structural, morphological, optical and electrical properties of PANi–ZnO nanocomposites. *Int J Polym Mater* 61:809–820
- Pawar SG, Patil SL, Mane AT, Raut BT, Patil VB (2009) Growth, characterization and gas sensing properties of polyaniline thin films. *Arch Appl Sci Res* 1(2):109–114
- Pawar SG, Patil SL, Chougule MA, Achary SN, Patil VB (2011) Microstructural and optoelectronic studies on polyaniline: TiO<sub>2</sub> nanocomposite. *Inter J Polym Mater* 60:244–254
- Perrin DD (2003) CRC Handbook of Chemistry and Physics, vol 1250, 84th edn. CRC Press, Boca Raton, p 1221
- Petriz RL (1956) Theory of photoconductivity in semiconductor films. *Phys Rev* 104:1508
- Pouget JP, Hsu CH, MacDiarmid AG, Epstein AJ (1995) Synthesis of iodine-capped aniline trimers and analysis of their electronic spectrum. *Synth Met* 69:119

- Quillard S, Corraze B, Boyer MI, Fayad E, Louarn G, Froyer G (2001) Vibrational characterization of crystallized oligianiline: a model compound of polyaniline. *J Mol Struct* 596:33–40
- Raut BT, Godse PR, Pawar SG, Chougule MA, Patil VB (2012a) New method for fabrication of polyaniline–CdS sensor for H<sub>2</sub>S gas detection. *Measurements* 45:94–100
- Raut BT, Godse PR, Pawar SG, Chougule MA, Sen S, Pawar RC, Lee CS, Patil VB (2012b) Novel method of fabrication of polyaniline–CdS nanocomposites: structural, morphological and optoelectronic properties. *Ceramic Inter J* 38:3999–4007
- Raut BT, Godse PR, Pawar SG, Chougule MA, Bandgar DK, Sen S, Patil VB (2012c) New process for fabrication of polyaniline–CdS nanocomposites: structural, morphological and optoelectronic investigations. *J Phys Chem Solids*. doi:10.1016/j.jpcs.2012.09.012
- Sajeev US, Mathai CJ, Saravanan S, Ashokan RR, Venkatachalam S, Anantharaman MR (2006) On the optical and electrical properties of rf and a.c. plasma polymerized aniline thin films. *Bull Mater Sci* 29:159–163
- Sekkina A, Tawfik A (1995) Further studies on the temperature dependence of the electric and photovoltaic properties of CdSe thin films for solar cells. *Thermochim Acta* 86:431–435
- Trchova M, Sedenkova I, Konyushenko EN, Stejskal J, Holler P, Ciric-Marjanovic G (2006) Polyaniline: the infrared spectroscopy of conducting polymer nanotubes. *J Phys Chem B* 110:9461–9468
- Trivedi DC (1997) In: Nalwa HS (ed) *Handbook of organic conductive molecules and polymers*, vol 2, issue no 2. Wiley, Chichester, p 505
- Vidotto G, Crosato-Arnaldi A, Talamini G (1969) Polymerization of acrylonitrile in the presence of different solvents. *Makromol Chem* 122:91–104
- Wang Y, Herron N (1991) Nanometer-sized semiconductor clusters: materials synthesis, quantum size effects and photophysical properties. *J Phys Chem* 95:525–532
- Xing S, Zhao C, Jing S, Wang Z (2006) Morphology and conductivity of polyaniline nanofibers prepared by ‘seeding’ polymerization. *Polymer* 47:2305–2313
- Zeng XR, Ko TM (1998) Structure and properties of chemically reduced polyaniline. *Polymer* 39:1187–1195
- Zhang Y, Xu W, Yao W, Yu S (2009) Oxidation–reduction reaction driven approach for hydrothermal synthesis of polyaniline hollow spheres with controllable size and shell thickness. *J Phys Chem C* 113(20):8588–8594